Available online at www.sciencedirect.com
ScienceDirect
Journal of Hazardous Materials 150 (2008) 238–249
Journal of Hazardous Materials
www.elsevier.com/locate/jhazmat

Degradation of cyanobacteria toxin by advanced oxidation processes

Fares Al Momani [a,*], Daniel W. Smith [b], Mohamed Gamal El-Din [b]

[a] *Department of Chemical Engineering, Mutah University, Jordan*
[b] *Department of Civil and Environmental Engineering, University of Alberta, Edmonton, Alberta, Canada T6G 2M8*

Received 6 September 2006; received in revised form 17 April 2007; accepted 19 April 2007
Available online 24 April 2007

Abstract

Advanced oxidation processes (AOPs) using O_3, H_2O_2, O_3/H_2O_2, O_3/Fe(II), and Fenton treatment were investigated for the degradation of aqueous solutions of cyanobacteria. The effects of concentration of reactants, temperature, and pH on toxins degradation were monitored and the reaction kinetics was assessed. O_3 alone or combined with either H_2O_2 or Fe(II) were efficient treatment for toxins elimination. A higher toxin oxidation tendency was observed with Fenton reaction; total toxins degradation (MC-LR and MC-RR) was achieved in only 60 s.

The ozonation treatment was successfully described by second-order kinetics model, with a first-order with respect to the concentration of either ozone or toxin. At 20 °C, with initial concentration of MC-LR of 1 mg/L, the overall second-order reaction rate constant ranged from 6.79×10^4 to 3.49×10^3 M^{-1} s^{-1} as the solution pH increased from 2 to 11. The reaction kinetics of the other AOPs (O_3/H_2O_2, O_3/Fe(II), and Fenton), were fitted to pseudo first-order kinetics. A rapid reaction was observed to took place at higher initial concentrations of O_3, H_2O_2 and Fe(II), and higher temperatures. At pH 3, initial concentration of toxin of 1 mg/L, the pseudo first-order rate constant, achieved by Fenton process, was in order of 8.76 ± 0.7 s^{-1}.

Keywords: Cyanobacteria; Fenton; Hydroxyl radical ($^{\bullet}$OH); Reaction rate constant

1. Introduction

Cyanobacteria toxins have quickly risen in infamy as important water contaminants that threaten human health [1]. Toxin introduce to the environment, in general, through the rupture of algal cells which may arise by the effect of certain substance used during water treatment [2] and/or during different water management processes, e.g. during algaecide treatment of the natural medium, pumping of raw water, conveyance of raw water.

Microcystins are a group of monocyclic heptapeptide hepatotoxins produced by various freshwater cyanobacteria such as *Microcystis*, *Anabaena*, *Nostoc* and *Oscillatoria* species [2]. The general structure of microcystins is cyclo[-D-Ala-L-*X*-D-MeAsp-L-*Z*-Adda-D-Glu-Mdha-]. Microcystins consist of three D-amino acids: alanine (Ala), methylaspartic acid (MeAsp) and glutamic acid (Glu), and two unusual amino acids: *N*-methyldehydroalanine (Mdha) and 3-amino-9-methoxy-2,6,8,-trimethyl-10-phenyldeca-4,6-dienoicacid (Adda). The Adda amino acid is responsible for the biological activity of the toxins. Microcystins differ primarily in the two L-amino acids, *X* and *Z*, which give its name to the molecule. There are more than 75 microcystin variants, and toxic strains usually produce a mixture of different microcystins [3,4]. MC-LR, with leucin L and arginin R residues, is the most common one. Owing to the production of these hepatotoxins the occurrence of aquatic blooms of cyanobacteria is of worldwide concern [5]. The incidents of wild and domestic animal poisoning and human health problems attributed to exposure to cyanobacterial toxins have been well documented [6–11].

Cyanobacteria toxins, in particular hepatotoxins, once released to water, are relatively stable [12]. These toxins can cause irreversible danger to the liver and can lead either to rapid death or to long-term pathologies such as liver cancer [1]. Different studied were concerned with the stability of these toxins to determine how long after the cyanobacterial bloom the water constitutes a threat to all potential users. Harada [12] and Lahti et al. [13] showed that microcystins and nodularin are chemically stable and, if not diluted, can persist in water for several days or weeks after the bloom. The study performed by Jones and Orr [14] showed that after algaecide treatment of a heavy bloom of

* Corresponding author.
E-mail address: fares1233@mutah.edu.jo (F. Al Momani).

0304-3894/$ – see front matter © 2007 Published by Elsevier B.V.
doi:10.1016/j.jhazmat.2007.04.087

Nomenclature

$[H_2O_2]$	concentration of hydrogen peroxide at time "t" (mg/L or M)
$[H_2O_2]_i$	initial hydrogen peroxide concentration (mg/L or M)
k_1	pseudo first-order kinetic rate constants for direct oxidation (s^{-1})
k_1^*	kinetic rate constants for direct ozone oxidation ($M^{-1}\,s^{-1}$)
k_2	pseudo first-order kinetic rate constants for indirect oxidation (s^{-1})
k_2^*	kinetic rate constants for indirect radicals oxidation ($M^{-1}\,s^{-1}$)
K	overall second-order rate constant ($M^{-1}\,s^{-1}$)
K_a	apparent rate constant (s^{-1})
$[O_3]$	concentration of ozone at time "t" (mg/L or M)
$[O_3]_f$	final concentration of ozone (mg/L or M)
$[O_3]_i$	initial concentration of ozone (mg/L or M)
ΔO_3	ozone dose utilized in the reaction (mg/L or M)
$[^{\bullet}OH]$	concentration of hydroxyl radical at time "t" (mg/L or M)
t	reaction time (s)
$t_{1/2}$	experimental toxin half-life (s)
[toxin]	concentration of toxin at time "t" (mg/L or M)
$[toxin]_f$	final concentration of toxin (mg/L or M)
$[toxin]_i$	initial concentration of toxin (mg/L or M)
T	temperature (°C)
Z	molar reaction requirements

Microcystis aeruginosa, the released microcystins persisted in the water for 9 days and then rapidly disappeared. Toxin fading was attributed to different operational processes such as dilution by uncontaminated water masses, adsorption on particulate material, temperature and pH-dependent decomposition, photolysis, and biological degradation. The laboratory experiments of Cousins et al. [15] demonstrated that primary degradation of MC-LR in reservoir water occurred in less than 1 week. On the other hand, MC-LR was stable in de-ionized water for over 27 days and in sterilized reservoir water for over 12 days. The toxicity of these compounds coupled with their stability is of concern for water supply utilities. Therefore, elimination of such compounds in water treatment processes merits investigation.

Several studies have been carried out to remove dissolved toxins from different type of water. Rositano and Nicholson [16] used three coagulants (ferric sulphate, alum and polyaluminium chloride) to remove dissolved microcystin, but to no avail, there was virtually no toxin removal. The study by Craig and Bailey [17] showed that granular activated carbon was effective in the removal of cyanobacterial toxin. But, the carbon was exhausted with constant use in a relatively short time period. Different oxidizing agents such as chlorine, ozone, potassium permanganate, hydrogen peroxide and ozone in combination with hydrogen peroxide were also evaluated for their ability to destroy the toxins [16,18–21]. These oxidants were evaluated in laboratory scale experiments to determine their effects on toxins removal. Pure toxins, freeze-dried toxic material, toxic cultures and toxic natural live bloom material was used in these studied. The studies showed that the effectiveness of the oxidation processes in water treatment is dependent not only on the reactant concentration, but also on temperature, pH and ionic composition of the water being treated.

The present work was undertaken to investigate the oxidation of pure microcystins (MC-LR and MC-RR), with and without the presence on any natural organic matter (NOM), by advanced oxidation processes based on ozone. The specific objectives were: (1) to determine the proper oxidation conditions of these AOPs for maximizing toxins degradation; (2) to determine the reaction rate constants with respect to toxin degradation under different operational conditions of pH and temperature.

2. Materials and methods

2.1. Chemicals

All chemicals and solvents were analytical or high performance liquid chromatography (HPLC) grade. High purity water was obtained from a Milli®-Q system (Millipore Corporation, USA) fed by distilled water. The microcystin-LR (MC-LR) with (90%) purity was obtained from Sigma-Aldrich. Microcystin-RR (MC-RR) with (97%) purity was obtained from Alexis Corporation, USA. The Chemical structure of microcystin toxin and microcystin-LR is shown in Fig. 1. For phosphate buffer solution sodium phosphate monobasic (Fisher scientific), potassium phosphate (Fisher scientific), de-ionized water (Milli®-Q Millipore system with an 18 MΩ cm^{-1} resistivity), sodium hydroxide (NaOH) (Fisher scientific) and Phosphoric acid (Fisher scientific), were used. Reagents used in HPLC measurements solution were 10 mM ammonium acetate (Fisher scientific), actitonitril HPLC grade (Fisher scientific) and phosphoric acid.

2.2. Sample preparation

The procedure used in preparing aqueous solution of MC-LR and MC-RR was as follows: (1) toxin stock solutions were prepared by dissolving specific toxin weight in 2 mL of methanol (HPLC grade), then, (2) the working solution was prepared by diluting the concentrated stock solution with a phosphate buffer to achieve the desired concentration and pH (pH of 2, 4.5, 7, 9 and 11). The buffer solution pH was regulated using a 1N sodium hydroxide (NaOH) or 1 M phosphoric acid. The phosphate buffer solution was prepared using sodium phosphate monobasic, potassium phosphate, and Milli-Q® water, and pH was regulated using a 1N NaOH solution or 1 M phosphoric acid. Working cyanobacteria toxins samples were prepared within 48 h of experiments and stored at 4 °C.

2.3. Analytical methods

The concentrations of microcystins were determined by two methods; (1) absorbance measurements in the RS-SF reactor;

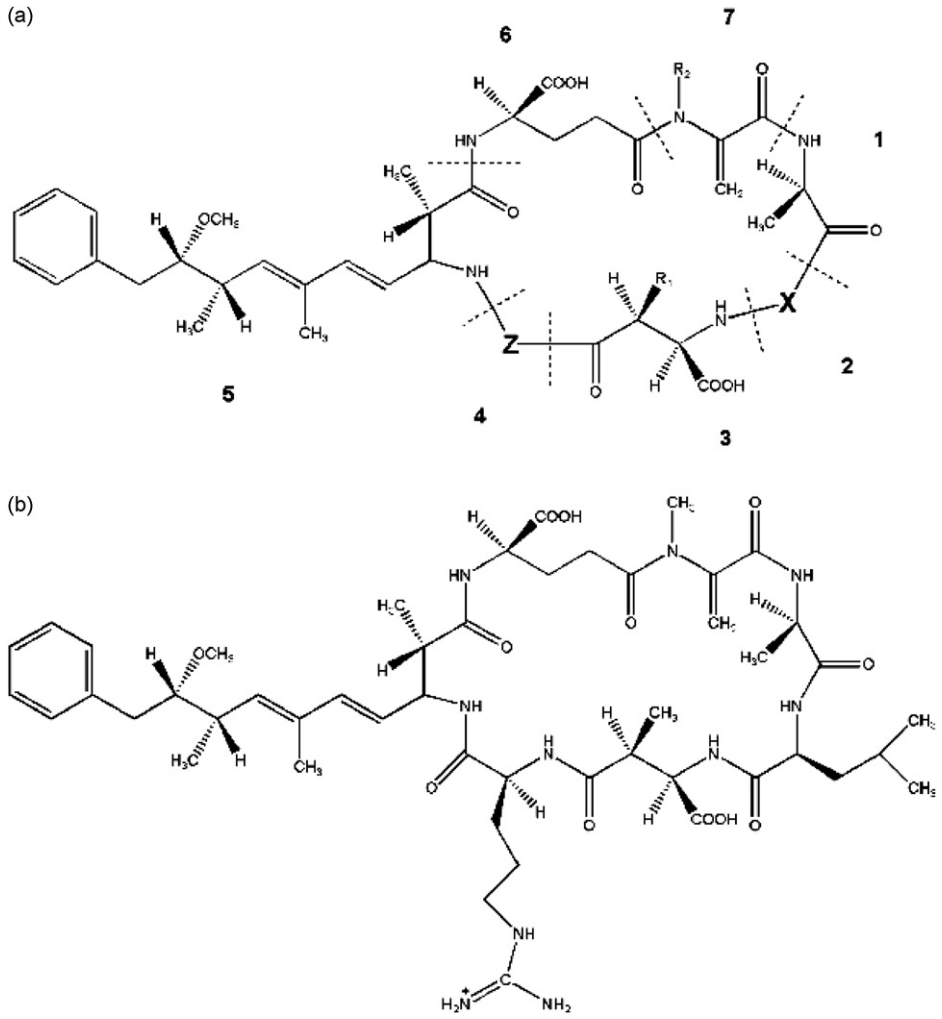

Fig. 1. (a) Generic structure of the microcystin toxin: 1, D-alanine; 2, *X* (variable); 3, D-MeAsp is D-erythro-β-methylaspartic acid; 4, *Z* (variable); 5, Adda is (2S,3S,8S,9S)-3-amino-9-methoxy-2,6,8-trimethyl-10-phenyldeca-4,6-dienoic acid; 6, D-glutamate; 7, Mdha is *N*-methyldehydroalanine (Dha, dehydroalanine). R1 and R2 are H (demethylmicrocystins) or CH_3. (b) Microcystin-LR, with the amino acid leucine in the variable *X* position and arganine in the *Z* position.

absorbance was measured in a wavelength range of 180–320 nm, and (2) by performing solid phase extraction followed by HPLC analysis. The extraction procedure was as follows: each aqueous toxin sample was filtrated through a pre-washed 0.45 μm Millipore membrane filter. The filtrate was then passed through a disposable 1 g C_{18} cartridges (Supelco) attached to vacuum chamber. The cartridges were prepared by washing them first with 10 mL acetonitrile and then 10 mL pure water. The aqueous toxin sample was passed through the cartridges at a rate of approximately 5 mL/min. The cartridges were then washed with 10 mL toxin free water. Next, the microcystin was then eluted with 5 mL of acetonitrile. The acetonitrile was evaporated to dryness under stream of nitrogen and the residue was then redissolved in acetonitrile 1 mL. A 20 μL sample was analyzed by HPLC. Microcystin concentrations were determined based on a standard curves (coefficient of single determination, $R^2 = 0.98$) obtained by plotting pure microcystin concentration against the peak height of the HPLC curve, different pure concentrations of microcystin were used in purpose. For each tested sample, measurements were repeated for 3 times to assure the data are reproducible, the obtained results were averaged, tested and it gave as maximum 7% standard deviation from the average value. HPLC analyses were performed with a Shimadzu liquid chromatograph (Shimadzu Scientific Instruments) equipped with Shimadzu pumps (model LC-10 AT) and a Shimadzu UV–vis detector (model SPD-10A). The reverse-phase column used was a C_{18}μ Bondapak (3.9 mm i.d. × 300 mm, Waters). The mobile phase was a mixture of 10 mM ammonium acetate and acetonitrile (65:35%) isocratically delivered by a pump at a flow rate of 1 mL/min. The wavelength of the UV absorbance detector was 238 nm. Under these conditions, the detection limit for microcystins was 0.2 μg/L. To assure analytical results the data obtained from HPLC and RS-SF were compared. The maximum difference obtained for several samples was <5%. Moreover, from time to time a pure microcystin sample, obtained from Sigma–Aldrich, was tested in our HPLC and RS-SF the results in both devices were same as specified from the manufacturer (difference <5%).

2.4. Ozone generation and dissolved ozone concentration measurements

An ozone generator model GLS-7 by PCI-WEDECO was used to produce ozone gas using extra dry, high purity oxygen. Dissolved ozone solutions were immediately prepared prior to ozonation experiments by bubbling ozone gas through pH phosphate buffer solutions (pH 2, 4.5, 7, 9, and 11) maintained at 4 °C to maximize ozone dissolution. Initial dissolved ozone concentrations entering the reactor and residual ozone concentrations in the rapid scan stopped-flow (RS-SF) reactor outlet were determined using two analytical methods: (1) a spectrophotometric measurement performed by RS-SF; (2) indigo method according to the procedure stipulated in *Standard Methods* [22]. The procedure to perform these measurements was as follow: the ozone solution was transferred from the bubbling bath via a 10 mL vile. To maintain the same ozone concentration, the 10 mL vile was kept in water bath at 4 °C. Then, two samples were taken from the vile with two pipettes and injected directly at the same time into an indigo solution and into the RS-SF reactor. The same procedure was followed for residual ozone measurement of outlet RS-SF solution. Also, another measurement was performed in a separate spectrophotometer to verify the previous measurement.

2.5. Advanced oxidation procedures

2.5.1. Degradation of toxins by ozonation

A multi-wavelength rapid scan stopped-flow (RS-SF) spectrophotometer system (Olis-Model 1000) was used to follow the oxidation kinetics during the ozonation of toxins in acidic and basic buffer solutions. This technique utilizes high resolution, high-speed double grating monochromators and thus, recording the reactant absorbance which can be related to chemical compound concentration, allows for the determination of reaction kinetic rates over a wide range of wavelengths. During the oxidation experiments, the evolution of the absorbance of the reactants over a wavelengths range of 180–320 nm was recorded as a function of time. MC-LR and MC-RR were found to have a maximum absorbance at 238 and 203 nm, respectively. Ozone has maximum absorbance at 260 nm. Thus, the selected wavelength range (180–320 nm) can be used to monitor the decay in ozone and toxins absorbance (i.e. ozone and toxins concentrations) as an indication of the progress of the oxidation reaction and toxins degradation. The ozonation experiments were conducted with initial ozone concentration ranged from 0.5 to 2 mg/L and pHs of 2, 4.5, 7, 9, and 11. The initial concentrations of toxins used in these oxidation experiments were 1, 2.5 and 5 mg/L for MC-LR and for MC-RR were 1 and 1.5 mg/L. The dead time of the instrument was determined to be 1.10 ± 0.01 ms. At the beginning of each experiment, the background absorbance was set to zero using the phosphate buffer solution as a reference. The two reactant solutions, prior to mixing, and the mixed solution were maintained at a pre-set temperature achieved by water circulation in a Julabo® thermostatic water bath. At the start of each experiment, the two aqueous solutions (one containing dissolved ozone and the other containing toxins) having the same pH, were rapidly mixed in the mixing cell of the RS-SF spectrophotometer system. Immediately after the rapid mixing, the solution absorbance at various reaction times was recorded. For each set of operational conditions, five identical experiments were conducted.

2.5.2. Kinetic data fitting

During ozonation experiments, the evolution of each reactant absorbance over a range of 180–320 nm was recorded as a function of reaction time. Five hundred data points (of the raw spectra) were recorded for each trace. The spectra were separated from noise using the Oliss singular value decomposition (SVD) software to identify the kinetically distinct species [23,24]. The number of the recorded kinetic data was then reduced to one fifth (100 data points) using the OlisTM smoothing algorithm. At least, five experiments were carried out for each set of experimental conditions. As a result, a total of 500 kinetic data points was obtained after smoothing the raw kinetic data from the five kinetic traces. These kinetic data were then averaged and were used to select the reaction mechanism(s). Following that, the averaged kinetic data were fitted to the optimal kinetic model using the Oliss SVD software. The pseudo first-order kinetic rate constants, used to model the MC-LR and MC-RR oxidation during ozonation, were determined at a 95% confidence level.

2.5.3. Degradation of toxins by H_2O_2, O_3/H_2O_2, O_3/Fe(II) and Fenton process

The working solutions of toxins in a phosphate buffer solution at different pHs (pH 2, 4.5, 7, and 11), were allowed to react with aqueous solutions of H_2O_2, O_3/H_2O_2, or O_3/Fe(II). The aqueous solutions of H_2O_2/O_3 and O_3/Fe(II) were prepared using an Olis stopped-flow pre-mixer. For each experiment, an aqueous solution of hydrogen peroxide or ferrous ion (initial concentration varied from 0.15 to 1.8 mg/L for Fe(II) and from 0.001 to 0.01 mg/L for H_2O_2) was mixed with ozonated water to give an initial ozone concentration somewhere in the range of 0.1–0.05 mg/L. The mixture was immediately allowed to react with the toxins solution in the mixing cell of the RS-SF reactor. Whenever possible, the absorbance decay of the reactants' concentrations was monitored over a wavelength range of 180–320 nm using Olis monochromators. The three solutions, prior to mixing, and the mixed solution were maintained at a pre-set temperature achieved by water circulation in a Julabo® thermostatic water bath. At the end of the 90-s reaction time, samples were taken and analyzed. The determination of initial and final hydrogen peroxide concentrations was carried out using the iodometric titration method described by Vogel [25]. The same mixing procedure used in the H_2O_2/O_3 and O_3/Fe(II) experiments was used to mix H_2O_2, Fe(II) and toxins during the toxins degradation using the Fenton process.

3. Results and discussion

3.1. Degradation of microcystin-LR (MC-LR) and microcystin-RR (MC-RR) by ozonation

Ozonation reaction is considering one the most powerful oxidants used in water treatment, having a standard oxidation

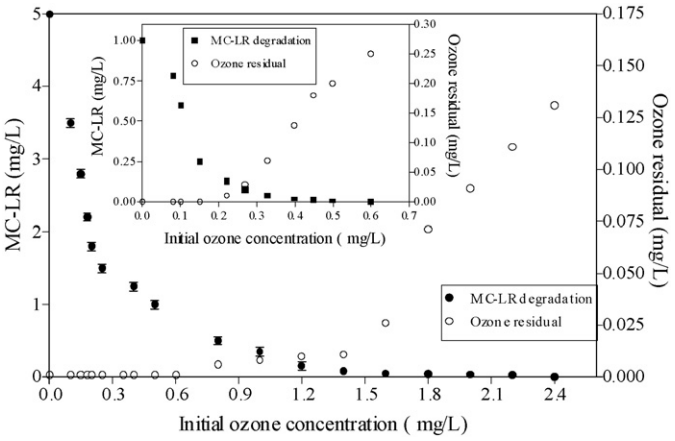

Fig. 2. Evolution of microcystin-LR concentration as a function of initial ozone concentration (temperature = 20.0 ± 0.2 °C, pH 7 and reaction time 90 s). Results are average of five repeated experiments performed at the same conditions.

potential of 2.07 V under acidic conditions. The ozonation of MC-LR and MC-RR by ozone was found to be effective under high initial ozone concentration. This was noticed in the reaction of pure toxins (MC-LR and MC-RR) and ozone. Fig. 2 illustrates the oxidation of different initial concentration of MC-LR (5.0 and 1.0 mg/L) with ozone. A solution containing a specific concentration of microcystin-LR (5 and 1.0 mg/L) was oxidized to below detection limit (0.2 μg/L) by used ozone dosage of 2 mg/L and reaction time less than 90 s. MC-LR with initial concentration of 5 mg/L was totally eliminated with initial ozone concentration of 2.4 mg/L, ozone residual and used ozone were 0.13 and 2.27 mg/L, respectively. Moreover, MC-LR with initial concentration of 1.0 mg/L was eliminated with initial ozone concentration of 0.6 mg/L (used ozone of 0.25 mg/L).

Similar trends were found with respect to MC-RR (Fig. 3; results are average of five repeated experiments performed at the same conditions). Two concentrations of MC-RR were studied (1.0 and 1.5 mg/L). Ozone is an efficient treatment process for elimination of MC-RR from water. For both initial concentrations studied, ozone in dose of 1.0 mg/L was sufficient to degrade the toxin to below detection limit (0.2 μg/L). For MC-RR concentration of 1.0 mg/L, there was a modest trend indicating a significant increase in the degradation efficiency of the MC-RR with increasing the ozone dose from 0.1 to 0.75 mg/L, after while ozone residual was detected in the solution, demonstrating excess in the used ozone dose (outer graph in Fig. 3). A degradation efficiency of more than 99% was obtained by used ozone dose of 0.7 mg/L. The same affinity was observed for MC-RR concentration of 1.5 mg/L, total toxin elimination was achieved with initial ozone dose of 1.1 mg/L and used ozone dose of 1.02 mg/L.

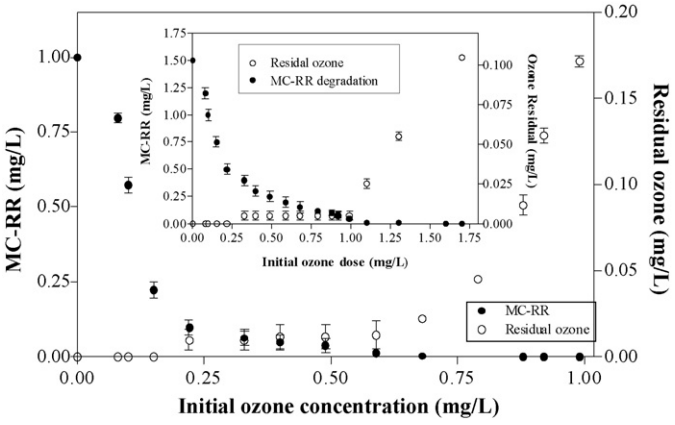

Fig. 3. Evolution of microcystin-RR concentration as a function of initial ozone concentration (temperature = 20.0 ± 0.2 °C, pH 7 and reaction time 90 s). Results are average of five repeated experiments performed at the same conditions.

The tendency of ozone in destruction MC-LR and MC-RR could be attributed to high ozone reactivity towards unsaturated bonds. Accordingly, the double bonds in the Adda group in microcystin would be prone to such attack. As microcystin toxicity is associated with the Adda olefin group, cleavage of this amino group would render the molecule non-toxic [2,26]. The same tendency reported in this study was confirmed by several authors [18–20,27].

In general, microcystin does not present, in nature, alone as pure compound, but it can be found mixed with other natural organic matter (NOM). When other organic material is introduced into the reaction, such as with reaction of ozone with MC-LR in the presence of natural organic matter (NOM), increased ozone dose were required to oxidize any toxin present. The NOM was achieved by dissolving humic acid in high purity water. The water pH was adjusted, to required pH, by 0.1 N NaOH solution. Once all the humic acid was dissolved in water, the solution was filtrated through a 45 μm Millpore filter paper. After that the solution was used to prepare solutions with different dissolved organic carbon (DOC) values by diluting the humic acid stock solution with appropriate water volumes. Fig. 4 presents the oxidation of toxines (MC-LR and MC-RR), initial concentration 1 mg/L, in the presence of different concentration of NOM as function of initial ozone dose. There was a direct relation between the toxin degradation and the presence of NOM. It can be summarized, therefore, that competing reactions occurred between the organic material and the toxin for reaction with ozone. Nevertheless, with initial ozone concentration of 0.6 mg/L up to 77% MC-LR and 75% MC-RR degradation can be achieved in the presence of 2 mg/L NOM within 90 s reaction (Fig. 4).

The effect of pH on the toxin oxidation efficiency was investigated (Fig. 5). It was observed that the oxidation reaction is highly dependent on the initial solution pH: as the pH was increased the degradation efficiency was decreased. The less effective oxidation at higher pH values reflects the lower oxidation potential of ozone under alkaline conditions (1.24 V) compared with that under acidic conditions (2.07 V). As it is well known that, ozone decomposition is accelerated under alkaline conditions by the presence of hydroxide ions which acts as radical initiators, the $HO^{\bullet}$ and O_2^- radicals which act as propagators, in a series of chain reactions. The fact that pure microcystins react much faster with ozone in acidic pH range suggests that microcystins probably react with ozone as opposed to hydroxyl radicals. Rositano et al. [28] reported that the toxin destruction efficiency depends on the pH and it is less favorable at alkaline conditions. This was due to lower ozone

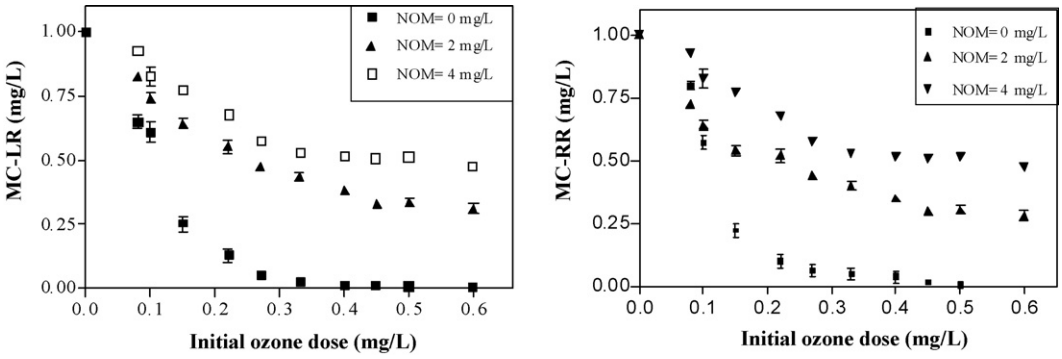

Fig. 4. Ozonation of microcystin (MC-LR and MC-RR) in the presence of NOM, average of five repeated experiments (temperature = 20.0 ± 0.2 °C, pH 7 and reaction time 90 s).

oxidizing potential at high pH. The same observation was confirmed by Shawwa and Smith [21], where at 20 °C, the overall reaction rate constant between ozone and MC-LR decreased from 1.0×10^5 to 3.4×10^4 M^{-1} s^{-1} as the pH increased from 2 to 7.

The effect of temperature on ozonation of MC-LR and MC-RR solutions were also studied (Fig. 5). Results illustrate that increasing reaction temperature leads to increase the oxidation reaction between ozone and microcystins, and hence increase the fraction of toxin removed. With used ozone of 1.0 mg/L, as the reaction temperature increased from 20 to 35 °C, MC-LR removal increased from 67 up to 87%. The same trends were observed with other experiments performed with MC-RR at different used ozone dose (results not shown). The degradation efficiency of MC-RR ranged from 78 to 95% at operational temperature range from 20 to 35 °C and used ozone dose ranged between 0.8 and 1 mg/L.

3.2. Kinetics of ozonation process

Before starting with kinetic measurements, a set of experiment was performed to study the reaction requirements. The aim of this part was to determine the number of moles of ozone needed to degrade one mole of toxin. For this purpose the ozonation reaction was performed in the RS-SF reactor for 120 s according to the procedure presented before. The previous steps were repeated 5 times for more than 5 initial ozone concentrations, and the reaction requirements were calculated according to Eq. (1):

$$\text{Reaction requirements } (z) = \frac{[O_3]_i - [O_3]_f}{[\text{toxin}]_i - [\text{toxin}]_f} \quad (1)$$

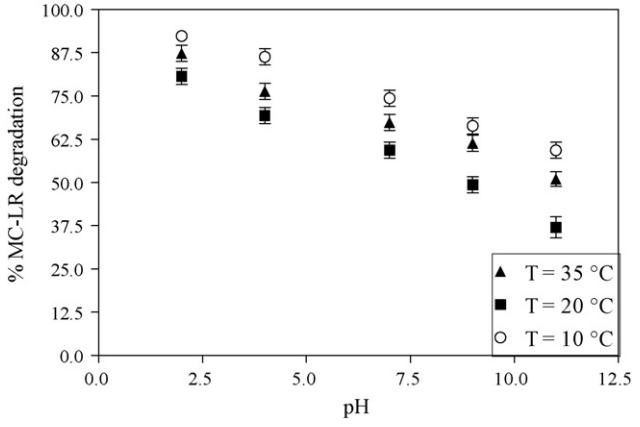

Fig. 5. Effects of pH and temperature on the degradation efficiency of MC-LR, average of five repeated experiments (initial ozone concentration = 0.25.8 mg/L, and reaction time of 90 s).

Calculations showed that, a value of 6 moles of ozone were required for oxidation of 1 mole of MC-LR and MC-RR. Results were calculated for 25 experiments with 95% confidence level. Standard deviation of the mean value and each separate experiment was as maximum 8%.

The rapid scan multi-wavelength stopped-flow (RS-SF) spectrophotometer system (Olis-Model 1000) was utilized to study the fast oxidation reaction between ozone and cyanobacteria in acidic and basic buffered solutions. During the oxidation experiments, the evolution of reactant absorbance (i.e. concentration), over a whole range of wavelengths (180–320 nm), was recorded as a function of time.

The oxidation experiments were carried out at different O_3/toxin molar ratio. The used O_3/MC-LR molar ratios were 1.92, 3.84, 7.69, 9.64, 15.37 and 38.58 while the molar ratios of O_3/MC-RR were 7.18, 10.84, 28.74 and 43.40. The initial solution pH was 2, 4.5, 7 and 11. The initial concentrations of toxin used in these reactions were 5, 2.5 and 1.0 mg/L for MC-LR while MC-RR initial concentration was 1.5 and 1.0 mg/L. At each reaction conditions, five identical experiments were performed.

The used O_3/toxin molar ratio in this study allows studying the reaction kinetic under (1) excess ozone concentration (i.e. toxin limiting concentration) and (2) low ozone concentration (i.e. ozone limiting concentration).

For the experiments performed under excess ozone (molar concentration ratio of ozone to toxins ≥10), it was observed that the absorbance decay of toxin could be described by two pseudo first-order decay rates. This tendency was attributed to direct molecular ozone oxidation and indirect hydroxyl free radicals oxidation; with domination of hydroxyl radical oxidation at pH > 7, and molecular ozone oxidation at pH < 7. As a result, the rate of toxins degradation could be described using a parallel

Table 1
The values of k_1, k_2 and K_a for MC-LR at different pH and different operational temperature; $[O_3]_i = 2$ mg/L

pH	T (°C)	MR-LR								
		1 mg/L			2.5 mg/L			5 mg/L		
		k_1[a]	k_2[a]	K_a[b]	k_1[a]	k_2[a]	K_a[b]	k_1[a]	k_2[a]	K_a[b]
	20	12.25	4.00	12.25	3.17	0.02	3.17	0.92	0.02	0.92
2	30	21.45	7.00	21.45	4.6	0.70	4.6	1.26	0.05	1.26
	35	27.88	7.00	27.88	4.78	0.20	4.78	1.57	0.08	1.57
	20	16.50	3.00	16.50	2.38	0.80	2.38	4.29	1.00	4.29
4.5	30	17.64	5.00	17.64	3.56	0.70	3.56	11.43	2.00	11.43
	35	18.96	4.00	18.96	4.55	0.90	4.55	18.48	3.00	18.48
	20	9.90	–[c]	9.90	0.51	–[c]	0.51	3.63	–[c]	3.63
7	30	10.46	–[c]	10.46	0.72	–[c]	0.72	5.71	–[c]	5.71
	35	14.22	–[c]	14.22	0.93	–[c]	0.93	6.63	–[c]	6.63
	20	0.05	0.62	0.62	–[c]	0.003	0.003	–[c]	0.002	0.002
11	30	0.02	1.80	1.80	–[c]	0.003	0.003	–[c]	0.010	0.01
	35	0.04	2.27	2.27	–[c]	0.005	0.005	–[c]	0.014	0.014

[a] Average of five experiments carried out at the same conditions.
[b] Kinetic data after a single value decomposition (SVD).
[c] The absorbance decay data was described by a single first-order decay rate.

bi-molecular rate expression:

$$-\frac{d[toxin]}{dt} = k_1[toxin] + k_2[toxin] \quad (2)$$

Consequently, in Eq. (2), the value of k_1 include the oxidation capacity of the available molecular ozone at time "t". Meanwhile, the value of k_2 include the oxidation capacity of the available hydroxyl radical at time "t". Hence, Eq. (2) can be rewritten as follow:

$$-\frac{d[toxin]}{dt} = k_1^*[toxin][O_3] + k_2^*[toxin][^\bullet OH] \quad (3)$$

The units of k_1^* and k_2^* is $M^{-1}\ s^{-1}$, i.e. second-order kinetic, this indicates that both the direct (ozone) and indirect (hydroxyl radical) concentration and the toxins concentration affect the reaction kinetic. As it is known that under basic conditions ozone decomposes to produce mainly hydroxyl radicals ($^\bullet$OH). k_1 and k_2 are related to k_1^* and k_2^* through the following equations:

$$k_1 = k_1^*[O_3] \quad (4)$$

$$k_2 = k_2^*[^\bullet OH] \quad (5)$$

Tables 1 and 2 show the experimental values of k_1 and k_2 obtained at a high initial ozone concentration, different operational temperature, different solution pHs and different initial toxin concentrations. High effect of initial solution pH on the reported rate constants (k_1 and k_2) was observed; as the solution pH increased from 2 to 11, the obtained values of k_1 and k_2 varied indicating that hydroxyl radicals' oxidation dominated over the molecular ozone oxidation. The effect of oxidation reaction operational temperature on the kinetic constants can also observe in Tables 1 and 2. Increasing the operational temperature led to an increase in the reaction rate constants. In Tables 1 and 2, two general observations can be noted; (1) at an initial pH 7, the recorded absorbance data of the toxins was described by only a single first-order decay rate; (2) based on the solution pH, there was a significant difference between the reported values of k_1 and k_2. These observations can be explained by the fact that under all the operational pHs both oxidation pathways (direct and indirect) are of importance [29]. However, a limiting step determines the global kinetic. With respect to the unique k_1 value obtained at pH 7, the mechanism showed that the free-radical initiating is the rate-determining step in the reaction [30]. Thus, a unique reaction rate constant could be achieved.

The kinetic date (Tables 1 and 2) were treated mathematically using the SVD algorithm (kinetic data fitting), the produced kinetic relationship gave values of one kinetic constant (values of K_a; Tables 1 and 2). This finding was due to (1) the small value of the second kinetic constant which may assumed negligible by

Table 2
The values of k_1, k_2 and K_a for MC-RR at different pH and different operational temperature; $[O_3]_i = 2$ mg/L

pH	T (°C)	MR-RR					
		1.0 mg/L			1.5 mg/L		
		k_1[a]	k_2[a]	K_a[b]	k_1[a]	k_2[a]	K_a[b]
	20	23.75	6.00	23.75	3.17	0.02	3.17
2	30	33.25	4.00	33.25	4.60	0.7	4.60
	35	36.75	3.00	36.75	4.78	0.2	4.78
	20	20.50	3.00	20.50	2.38	0.8	2.38
4.5	30	22.25	5.00	22.25	3.56	0.7	3.56
	35	28.00	4.00	28.00	4.55	0.9	4.55
	20	20.00	–[c]	20.00	0.51	–[c]	0.51
7	30	25.00	–[c]	25.00	0.72	–[c]	0.72
	35	25.00	–[c]	25.00	0.93	–[c]	0.93
	20	0.01	0.07	0.07	–[c]	0.62	0.62
11	30	0.02	0.09	0.09	–[c]	1.80	1.80
	35	0.04	0.09	0.09	–[c]	2.27	2.27

[a] Average of five experiments carried out at the same conditions.
[b] Kinetic data after a single value decomposition (SVD).
[c] The absorbance decay data was described by a single first-order decay rate.

Table 3
The overall second-order rate constant (K) obtained during ozonation of MC-LR at different pHs and temperatures

pH	$K \times 10^{-2}$ (M^{-1} s^{-1}; $[MC\text{-}LR]_i = 1.0$ mg/L)			$K \times 10^{-2}$ (M^{-1} s^{-1}; $[MC\text{-}LR]_i = 2.50$ mg/L)			$K \times 10^{-2}$ (M^{-1} s^{-1}; $[MC\text{-}LR]_i = 5$ mg/L)		
	20[a]	35[a]	35[a]	20[a]	35[a]	35[a]	20[a]	35[a]	35[a]
2	679.00	1090.00	1420.00	161.00	234.00	239.00	400.00	681.00	7690.00
4.5	839.00	984.00	964.00	121.00	181.00	231.00	221.00	611.00	995.00
7	503.00	532.00	723.00	25.800	37.60	47.400	195.00	308.00	357.00
11	349.00	106.00	133.00	0.138	0.184	0.232	0.104	0.575	0.995

[a] Temperature (°C).

the mathematical program, and (2) the proper kinetic, assumed by the mathematical algorithm, is pseudo first-order. According to experimental finding, Eq. (3) can be rearranged as follows:

$$-\frac{\mathrm{d[toxin]}}{\mathrm{d}t} = (k_1^*[O_3] + k_2^*[^\bullet OH])[\mathrm{toxin}] \quad (6)$$

Therefore, for small reaction time and high O_3/toxin molar ratio, the terms $(k_1[O_3] + k_2[^\bullet OH])$ could be replaced by a constant, K_a:

$$-\frac{\mathrm{d[toxina]}}{\mathrm{d}t} = K_a[\mathrm{toxin}] \quad (7)$$

The previous assumptions are valid for three reasons:

1. the short time used in recording the kinetic data (absorbance decay was occurred during 90 s) that implies the presence of sufficient concentrations of ozone and hydroxyl radicals;
2. the used initial ozone dose (molar concentration ratio of ozone to toxin > 10) was higher than the toxin requirements, indicating the presence of excess ozone;
3. ozonation reaction is known to behave as second overall kinetic with first-order for each of the reactants [31].

With respect to ozonation reactions performed with low O_3/toxin molar ratios ≤10 (i.e. toxin is in excess), it was observed that ozone consumed rapidly in the reaction medium and the degradation efficiency of the toxin levelled off. The recorded absorbance data of ozone (at wavelength 260 nm) was treated with Olis algorithm and the data was fitted easily to a first-order kinetic model.

From the tendency observed during the two sets of experiments; high O_3/toxin molar ratios and low O_3/toxin molar ratio, it was observed that both toxin initial concentration and ozone initial concentration has a direct effect of the ozonation treatment kinetics. Consequently, the overall reaction rate constant between ozone and toxin could be described using a second-order kinetic model with respect to the concentration of both reactants (Eq. (8)):

$$-\frac{1}{z}\frac{\mathrm{d[toxin]}}{\mathrm{d}t} = -\frac{\mathrm{d}[O_3]}{\mathrm{d}t} = K[O_3]^n[\mathrm{toxin}]^m \quad (8)$$

where n and m are the reaction orders with respect to ozone and toxin, respectively. Comparing Eq. (7) with Eq. (8) indicates that k_a and K are related through the following equation:

$$k_a = \frac{1}{z}K[O_3]^n \quad (9)$$

This equation is valid under the condition where the ozone concentration in the solution was presumably unchanged (i.e. experiments that were conducted with ozone in excess). Under the present experimental condition both n and m were found to be equal 1 (the decay in absorbance data was fitted to first-order exponential decay). Thus, Eq. (9) reduced to:

$$K = \frac{zk_a}{[O_3]} \quad (10)$$

The overall second-order rate constant (K) was calculated based on the pseudo first-order rate constant, the reaction requirements and initial dissolved ozone concentrations over a temperature range of 20–35 °C (Eqs. from (8) to (10)). The calculated individual K values, obtained at the same pH and temperature, were averaged to give the averaged overall second-order rate constant. The maximum deviation of the averaged overall second-order rate constant from the calculated individual K values was found to be 5%.

Tables 3 and 4 summarize the overall rate constant (K) obtained at different experimental conditions for the ozone oxidation reaction of MC-LR and MC-RR. Tabulated values illustrate the effect of pH, temperature and initial toxin concentration on the overall rate constant K (M^{-1} s^{-1}). At 20 °C, increasing the solution pH from 8 to 11, was led to decrease in K value by a factor of five for MC-LR and a factor of three for

Table 4
The overall second-order rate constant (K) obtained during ozonation of MC-RR at different pHs and temperatures

pH	$K \times 10^{-2}$ (M^{-1} s^{-1}; $[MC\text{-}RR]_i = 1.0$ mg/L)			$K \times 10^{-2}$ (M^{-1} s^{-1}; $[MC\text{-}RR]_i = 1.5$ mg/L)		
	20[a]	30[a]	35[a]	20[a]	30[a]	35[a]
2	2450.00	2700.00	2970.00	397.00	587.00	700.00
4.5	1230.00	1350.00	1480.00	389.00	395.00	510.00
7	167.00	209.00	28.00	363.00	456.00	560.00
11	0.50	0.55	0.55	1.31	151.00	1.51

[a] Temperature (°C).

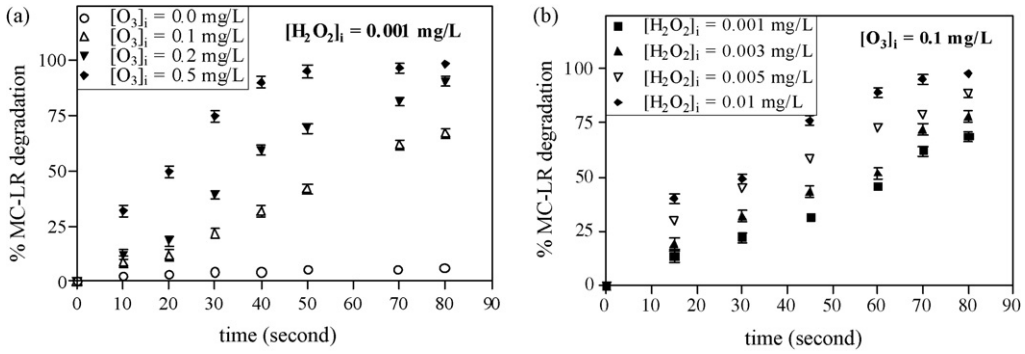

Fig. 6. Degradation efficiency of aqueous solution of MC-LR of initial concentration of 1 mg/L by O_3/H_2O_2 process at different initial concentrations of ozone and H_2O_2 (pH 7, temperature = 20 °C). Results are average of five repeated experiments performed at the same conditions.

MC-RR. Shawwa and Smith [21] studied the oxidation kinetic of MC-LR by ozone. Reported rate constant are in agreement with values obtained in the present study.

3.3. Degradation of toxin by H_2O_2, O_3/H_2O_2 and O_3/Fe(II)

From the previous results, one may be concluded that once the ozone demand of the water has been met, complete removal of toxin can be achieved. However, the effectiveness of ozone as an oxidant in the water treatment is dependent not only in the concentrations of reactants, but also temperature, pH and type of water being ozonated (water matrix).

Another technique for accelerating the oxidation reaction is the addition of either hydrogen peroxide (reactions (1′) and (2′) shown below) or iron ions (reactions (3′) and (4′) shown below) to the ozonated solution. Hydrogen peroxide in aqueous solution is partially dissociated to hydroperoxide anion (HO_2^-), which reacts with ozone giving rise to a series of chain reactions including hydroxyl radicals (as shown in reactions (1′) and (2′)). On the other hand, iron ions are considered to increase the number of hydroxyl radicals formed through the reduction of O_3 with the Fe^{2+} [32], a process similar to the mechanism proposed for the photo-Fenton reaction (reactions (3′) and (4′) shown below).

$$H_2O_2 + 2O_3 \rightarrow 2^{\bullet}OH + 3O_2 \quad (1')$$

$$HO_2^- + O_3 \rightarrow HO_2^{\bullet} + O_3^{\bullet} \quad (2')$$

$$Fe^{2+} + O_3 \rightarrow FeO^{2+} + O_2 \quad (3')$$

$$FeO^{2+} + H_2O \rightarrow Fe^{3+} + {}^{\bullet}OH + OH^- \quad (4')$$

Fig. 6 presents the results obtained during the oxidation of MC-LR (initial concentration of 1 mg/L) at different initial concentrations of ozone and H_2O_2. Although hydrogen peroxide alone, at an initial concentration of 0.001 mg/L, did not lead to considerable toxin degradation; less than 5% degradation efficiency (Fig. 6a), when combined with O_3, the degradation efficiency was increased. At a fixed initial H_2O_2 concentration of 0.001 mg/L (Fig. 6a), increasing the initial ozone concentration led to an increase in MC-LR degradation efficiency, as more than 98% of toxin was degraded with a 80 s reaction time and an initial ozone concentration of 0.5 mg/L (amount of used ozone being 0.2 mg/L). Moreover, at a fixed initial ozone concentration of 0.1 mg/L and different initial H_2O_2 concentrations (Fig. 6b), MC-LR degradation ranged from 65 to 95% as H_2O_2 initial concentrations increased from 0.001 to 0.005 mg/L. Complete MC-LR degradation was achieved in 80 s with an initial H_2O_2 concentration of 0.01 mg/L. The observed tendency could be attributed to the reaction involving hydrogen peroxide and ozone leading to more oxidative environment. Similar trends were observed for experiment performed with MC-RR (results not shown); more than 95% of MC-RR was degraded in 80 s reaction time with initial ozone concentration of 0.15 and 0.005 mg/L H_2O_2. Complete MC-RR degradation was achieved in 80 s with an initial ozone concentration of 0.4 mg/L and an initial H_2O_2 concentration of 0.01 mg/L.

The O_3/Fe(II) process was also tested for toxins degradation. In the O_3/Fe(II) process, not only the dissolved ozone led to toxin degradation, but the ferrous ion also underwent a redox reaction producing more hydroxyl radicals. Fig. 7 presents the experimental data obtained during MC-LR degradation using the O_3/Fe(II) process. Combining ferrous ion (Fe(II)) with ozone was also an efficient treatment option for toxin degradation. At a fixed initial ozone concentration of 0.2 mg/L, the toxin degradation efficiency was improved by increasing the initial Fe(II) concentration from 0.05 to 0.25 mg/L. At an initial Fe(II) concentration of 0.25 mg/L, more than 99% of the MC-LR was

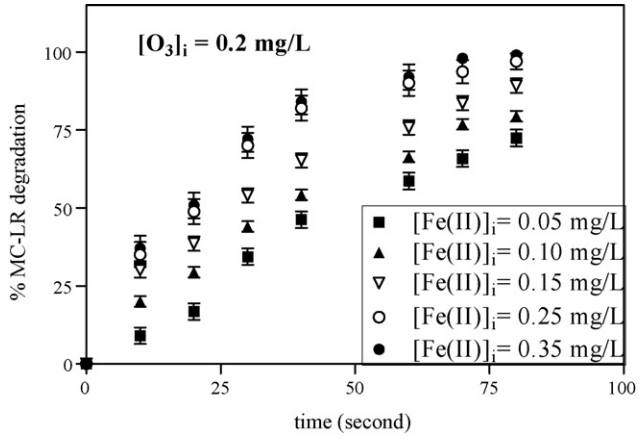

Fig. 7. Degradation efficiency of toxin (initial concentration of 1 mg/L) by means of O_3/Fe(II) process (pH 7, temperature = 20 °C, initial ozone concentration of 0.2 mg/L). Results are average of five repeated experiments performed at the same conditions.

degraded in 80 s reaction time. The difference, in terms of the amount of hydroxyl radicals formed, between the oxidation capacity of the O_3/Fe(II) process and the ozone process, indicates that more hydroxyl radicals were formed as a result of ferrous ion redox reactions [33]. However, it was observed that increasing the initial iron concentrations (above 0.25 mg/L) did not lead to significant improvement in MC-LR degradation efficiency. The degradation tendency, at a ferrous ion concentration higher than 0.25 mg/L, could be attributed to the formation of several Fe(II)–hydroperoxy complexes, such as $Fe(HO_2)^{2+}$ and $Fe(OH)(HO_2)^{2+}$, which decompose to produce the hydroperoxy radicals $HO_2^{\bullet}$ and Fe(II). $HO_2^{\bullet}$, is relatively non-reactive with organic matter [34]. The same tendency was observed for MC-RR degradation; the oxidation efficiency increase by increasing Fe(II) initial concentration up to 0.2 mg/L and then the degradation efficiency level off. More than 99% MC-RR was degraded in 80 s with an initial concentration of 0.2 mg/L ozone and an initial concentration of 0.2 mg/L Fe(II).

3.4. Degradation of toxin by Fenton process

Fenton reagent, a mixture of ferrous ion (Fe(II)) and hydrogen peroxide which produces $^{\bullet}OH$ radicals (reaction (5′)), has been used extensively for the oxidation of organic matter, the reduction of chemical oxygen demand (COD), and total organic carbon (TOC) contents of wastewater [33,35].

$$Fe(II) + H_2O_2 \rightarrow Fe(III) + OH^{\bullet} + OH^{-} \quad (5')$$

The use of Fe(II)/H_2O_2 as an oxidant for wastewater is an attractive option as iron is highly abundant and non-toxic. Also, 30% hydrogen peroxide aqueous solution is easy to handle and environmentally friendly. MC-LR degradation by Fenton reaction at different initial hydrogen peroxide concentrations and different initial Fe(II) concentration are shown in Fig. 8. The Fenton process was efficient for the degradation of MC-LR. The degradation efficiency depended on the initial H_2O_2 concentration; increasing the initial concentration of H_2O_2 and maintaining the initial Fe(II) concentration constant was led to an increase in toxin degradation efficiency. A 100% MR-LR degradation was achieved in 80 s reaction time, initial concentration of Fe(II) of 0.05 mg/L and initial concentration of H_2O_2 of 0.02 mg/L (inner graph Fig. 8). Similar trends were observed for MC-RR (results not shown).

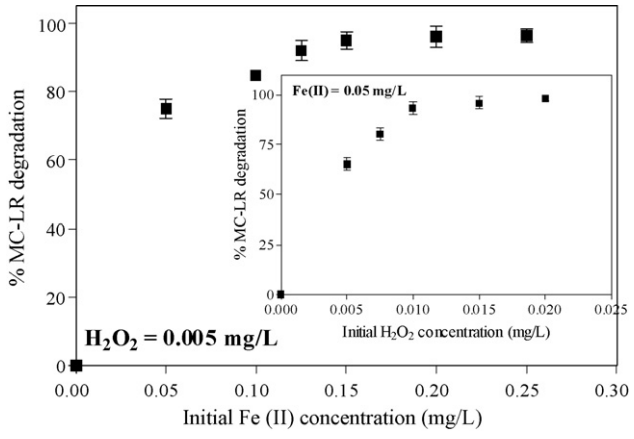

Fig. 8. Degradation efficiency of MC-LR (initial concentration of 1 mg/L) as a function of initial H_2O_2 and initial Fe(II) in Fenton process, average of five repeated experiments, conditions (pH 7, temperature = 20 °C, reaction time of 80 s).

To examine the effect of the initial concentration of Fe(II) on toxin degradation efficiency, experiments were carried out with variable initial Fe(II) concentration while the initial H_2O_2 concentration was maintained at 0.005 mg/L (outer graph of Fig. 8). It was observed that Fe(II) concentration had a positive effect on MC-LR degradation efficiency; up to 98% toxin degradation was achieved with an initial Fe(II) concentration of 0.2 mg/L. However, at initial Fe(II) concentrations higher than 0.2 mg/L, degradation efficiency did not change significantly (5% significance level). The Fenton process behavior, at high initial Fe(II) concentration, could be explained by the same hypothesis as that used to account for the O_3/Fe(II) process performance. Moreover, the catalytic effect of Fe(II) on the decomposition of H_2O_2 to H_2O and O_2 may also support this hypothesis [36].

The influence of other Fenton process operational conditions, such as initial pH, operating temperature and initial toxin concentration, on the degradation efficiency was also investigated. At initial reactant concentrations of 0.005 mg/L for H_2O_2 and 0.05 mg/L for Fe(II), as well as 80 s of reaction time, it was observed that MC-LR degradation efficiency increased as solution pH decreased. At an initial toxin concentration of 1 mg/L, decreasing the solution pH from 7 to 3 increased toxin degradation efficiency from 75 to 85%. The low oxidation capacity (i.e. low degradation efficiency) of the Fenton process at high pH values could be attributed to the partial decomposition of Fe(II) under basic conditions and/or to iron hydroxide precipitation [36].

It was also observed that the efficiency of toxin degradation increased with increasing operating temperatures. At initial reactant concentrations of 0.005 mg/L for H_2O_2 and 0.05 mg/L for Fe(II), as well as 80 s of reaction time, the MC-LR degradation efficiency increased from 60 to 84% when the temperature increased from 20 to 35 °C.

The rate of degradation was also found to be dependent on the initial toxin concentration. For an initial H_2O_2 concentration of 0.005 mg/L, an initial Fe(II) concentration of 0.05 mg/L and 80 s of reaction time, 75% of the MC-LR was degraded when an initial toxin concentration of 1 mg/L was used. Meanwhile, at the same initial concentrations of H_2O_2 and Fe(II), and an initial toxin concentration of 0.5 mg/L, a degradation efficiency of 97% was achieved. This oxidation tendency confirms the non-selectivity of the hydroxyl radical reaction for the degradation of toxin.

Similar trends were observed for the experiments carried out with MC-RR; both hydrogen peroxide and Fe(II) had a significant effect on MC-RR degradation, with an initial concentration of 0.005 mg/L H_2O_2, an initial Fe(II) concentration of 0.1 mg/L and 80 s of reaction time, 100% of 1 mg/L MC-RR was degraded (results no shown).

A comparison of the oxidation of toxin (mainly MC-LR) at an initial concentration of 1.0 mg/L with various oxidants is shown in Fig. 9 (presented data is the average of five repeated experi-

Table 5
Apparent rate constant (k_a, s^{-1}) and half-life ($t_{1/2}$, s) for both MC-LR and MC-RR by different oxidation processes

Process	MC-LR = 1 mg/L				MC-RR = 1 mg/L			
	$k_a \times 10^{-2}$ (s^{-1})[a]	Theoretical $t_{1/2}$ (s)	Expermental $t_{1/2}$ (s)	R^2	$k_a \times 10^{-2}$ (s^{-1})[a]	Theoretical $t_{1/2}$ (s)	Expermental $t_{1/2}$ (s)	R^2
Fenton[b]	8.76	8	9	98	9.56	7	8	95
O_3/H_2O_2[c]	5.25	13	17	93	6.00	12	14	97
O_3/Fe(II)[d]	4.77	14.5	18	96	5.20	13	15	95
H_2O_2[e]	0.094	737	>90	85	0.098	707	>90	95

[a] Average of five repeated experiment calculated at 90% confidence interval.
[b] Initial H_2O_2 concentration = 0.005 mg/L and initial Fe(II) concentration = 0.2 mg/L.
[c] Initial H_2O_2 concentration = 0.001 mg/L and initial O_3 concentration = 0.5 mg/L.
[d] Initial Fe(II) concentration = 0.25 mg/L and initial O_3 concentration = 0.2 mg/L.
[e] Initial H_2O_2 concentration = 0.001 mg/L.

ments at the same conditions). O_3/H_2O_2, O_3/Fe(II) and Fenton processes were effective for toxin degradation. Despite the fact that ozone alone, with an initial concentration of 2 mg/L, led to a 100% degradation of toxin in 90s, the combination of ozone (0.5 mg/L) with H_2O_2 at an initial concentration of 0.001 mg/L, or with Fe(II) at an initial concentration of 0.25 mg/L, led to 100% and 98% degradation efficiency of toxin, respectively, in 80 s reaction time. A higher oxidation tendency was observed for the Fenton process, using an initial H_2O_2 concentration of 0.005 mg/L and an initial Fe(II) concentration of 0.2 mg/L. This set of conditions led to complete degradation of the toxin in less than 50 s. The same tendency was observed in MC-RR degradation (result not shown).

3.5. Kinetic study of H_2O_2, O_3/H_2O_2, O_3/Fe(II) and Fenton process

The multi-wavelength rapid scan stopped-flow (RS-SF) spectrophotometer system (Olis-Model 1000) was used to study the kinetics of the oxidation reactions. Due to some difficulties in recording the absorbance decay for the aqueous solutions of H_2O_2 and Fe(II), it was decided to only follow the decay in the absorbance of toxin (at fixed wavelength of 238 nm for MC-LR and 308 nm for MC-RR). Thus, in this part of the study, only the apparent toxin decay rate constant (k_a) will be presented. These data were obtained from the reaction kinetic data fitting of the toxin absorbance using Oils kinetic algorithms.

Table 5 presents the values for the apparent decay rate constant (k_a, s^{-1}) and the experimental toxin half-life ($t_{1/2}$, s) for both MC-LR and MC-RR with initial concentration of 1 mg/L. The oxidation processes were carried out at same experimental conditions presented in Fig. 9 (average of five repeated experiments). The results confirm the significant (at 95% confidence level) acceleration effect the Fenton reactions on toxin degradation compared with other oxidation processes. Adding Fe(II) or H_2O_2 to the ozonated water showed a significant influence (at 90% confidence level) on the toxin degradation rate. The apparent decay rate constant of toxin was found to be 8.76 and 9.56 s^{-1} for MC-LR and MC-RR, respectively. The processes of O_3/H_2O_2 and O_3/Fe(II) had apparent decay rate constant in the same order of magnitude (Table 5).

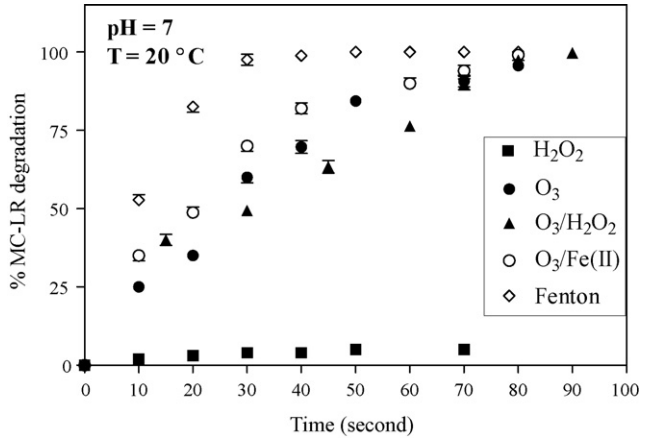

Fig. 9. A comparative oxidation of MC-LR by various oxidants, conditions pH 7, temperature = 20 ± 0.5, $[MC\text{-}LR]_i$ = 1 mg/L; (◊) initial concentration H_2O_2 = 0.001 mg/L; (▲) initial concentration H_2O_2 = 0.001 mg/L and initial concentration O_3 = 0.5 mg/L; (○) initial concentration Fe(II) = 0.25 mg/L and initial concentration O_3 = 0.2 mg/L; (●) initial concentration O_3 = 2 mg/L; (♦) initial concentration H_2O_2 = 0.005 mg/L and initial concentration Fe(II) = 0.2 mg/L. Results are average of five repeated experiments performed at the same conditions.

4. Conclusions

Advanced oxidation processes based on ozone (O_3/H_2O_2, O_3/Fe(II), and Fenton) were efficient for toxin degradation. The degradation rate was influenced by initial ozone concentration, initial hydrogen peroxide concentration, initial iron-ion concentration, initial pH and temperature. Fenton and O_3/H_2O_2 processes could be used successfully to achieve total toxin degradation. Total toxin degradation was obtained by the Fenton process in reaction time of 60 s, and with initial reactant concentrations of 0.005 mg/L H_2O_2 and 0.2 mg/L Fe(II).

The ozonation kinetic was performed by the stopped-flow spectrophotometry technique. The reaction between ozone and toxin could be modeled as second-order for both reactants, and as pseudo first-order for either the ozone or the toxin concentration. At 1 mg/L initial MC-LR toxin concentration and solution pH of 11, the overall reaction rate constant (K) varied from 3.49×10^3 to 1.33×10^4 M^{-1} s^{-1} in the temperature range from 20 to 35 °C. The reaction kinetics and half-life times for the other AOPs processes (O_3, H_2O_2, O_3/H_2O_2, O_3/Fe(II) and Fenton) were followed according to the decay in toxin apparent concen-

tration. Faster reactions took place at higher initial oxidizing agent concentrations and higher temperatures. At a pH value of 7, initial MR-LR toxin concentration of 1 mg/L, reagent concentrations of 0.005 mg/L for H_2O_2 and 0.2 mg/L for Fe(II), a first-order degradation constant of 8.76 s^{-1} and a half-life time of 9 s were obtained for the Fenton reaction. First-order constants of the same order of magnitude were obtained for the O_3/H_2O_2 and O_3/Fe(II) processes, 5.25 and 4.77 s^{-1}, respectively.

Acknowledgements

The authors gratefully acknowledge the financial support from the Natural Sciences and Engineering Research Council of Canada (NSERC), the Canada Foundation for Innovation (CFI), and the Alberta Ingenuity Fund (AIF).

References

[1] C. Svrcek, D.W. Smith, Cyanobacteria toxins and the current state of knowledge on water treatment options: a review, Environ. Eng. Sci. 3 (3) (2004) 155–185.
[2] W.W. Carmichael, A Status Report on Planktonic Cyanobacteria (Blue-green Algae) and their Toxins Summary Report, EPA/600/SR-92-079, Environmental Monitoring Systems Laboratory, Office of Research and Development, US EPA, Cincinnati, OH, 1992.
[3] K. Sivonen, G. Jones, Toxic cyanobacteria in water: a guide to their public health consequences, monitoring, and management, in: I. Chorus, J. Bartram (Eds.), Cyanobacterial Toxins, Published on behalf of the World Health Organization, E and FN Spon, New York, NY, 1999, pp. 41–111.
[4] L. Spoof, P. Vesterkvist, T. Lindholm, J. Meriluoto, Screening for cyanobacterial hepatotoxins, microcystins and nodularin in environmental water samples by reversed-phase liquid chromatography–electrospray ionisation mass spectrometry, J. Chromatogr. A 1020 (1) (2003) 105–119.
[5] T. Ohta, E. Sueoka, N. Iida, A. Komori, M. Suganuma, R. Nishiwaki, M. Tatematsu, S.J. Kim, W.W. Carmichael, H. Fujiki, Nodularin, a potent inhibitor of protein phosphatases 1 and 2A, is a newen vironmental carcinogen in male F344 rat liver, Cancer Res. 54 (1994) 6402–6406.
[6] S.G. Bell, G.A. Codd, Cyanobacterial toxins and human health, Rev. Med. Microbiol. 5 (4) (1994) 256–264.
[7] W.R. Harding, N. Rowe, J.C. Wessels, K.A. Beattie, G.A. Codd, Death of a dog attributed to the cyanobacterial (blue-green algal) hepatotoxin nodularin in south africa, Tydskr. S. A. fr.V et.V er. 66 (4) (1995) 256–259.
[8] K. Mez, K.A. Beattie, G.A. Codd, K. Hanselmann, B. Hauser, H. Naegeli, H.R. Preisig, Identification of a microcystin in benthic cyanobacteria linked to cattle deaths on alpine pastures in switzerland, Eur. J. Phycol. 32 (2) (1997) 111–117.
[9] M. Pliński, G.A. Codd, Cyanobacteria—a factor of animal intoxication: a review, Medycyna Wet. 53 (1) (1997) 8–10 (in Polish).
[10] S. Pouria, A. de Andrade, J. Barbosa, R.L. Cavalcanti, V.T.S. Barreto, C.J. Ward, W. Preiser, G.K. Poon, G.H. Neild, G.A. Codd, Fatal microcystin intoxication in haemodialysis unit in caruaru, Lancet 352 (1998) 21–26.
[11] G.A. Codd, S.G. Bell, K. Kaya, C.J. Ward, K.A. Beattie, J.S. Metcalf, Cyanobacterial toxins, exposure routes and human health, Eur. J. Phycol. 34 (1999) 405–415.
[12] K.-I. Harada, Chemistry and Detection of Microcystins, Toxic Microcystis, CRC Press/Boca Raton, New York/London/Tokyo, 1995, pp. 103–143.
[13] K. Lahti, J. Rapala, M. Fardag, N. Maija, K. Sivonen, Persistence of cyanobacterial hepatoxin, microcystin-lr, in particulate material and dissolved in lake water, Water Res. 31 (5) (1997) 1005–1012.
[14] G.J. Jones, P.T. Orr, Release and degradation of microcystin following algicide treatment of a Microcystis aeruginosa bloom in a recreational lake, as determined by HPLC and protein phosphatase inhibition assay, Water Res. 28 (4) (1994) 871–876.
[15] I.T. Cousins, D.J. Bealing, H.A. James, A. Sutton, Biodegradation of microcystin-LR by indigenous mixed bacterial populations, Water Res. 30 (2) (1996) 481–485.
[16] J. Rositano, B.C. Nicholson, Water Treatment Techniques for Removal of Cyanobacterial Toxins from Water, Australian Centre for Water Quality Research, Salisbury, South Australia, 1994, p. 55.
[17] K. Craig, D. Bailey, Cyanobacterial toxin microcystin-lr removal using granular activated carbon-hunter water corporation experience, in: Proceeding of the 16th Australian Water and Wastewater Association Federal Convention, AWWA Inc, Artarmon, NSW, 1995, pp. 579–586.
[18] A. Keijola, K. Himberg, A. Esala, K. Sivonen, L. Kiisvirata, Removal of cyanobacterial toxins in water treatment processes: laboratory and pilot plant experiments, Toxic. Assess. 3 (1988) 643–656.
[19] J. Fawell, J. Hart, H. James, W. Parr, Blue-green algae and their toxins: analysis, toxicity, treatment, and environmental control, Water Supply 11 (3–4) (1993) 109–121.
[20] J. Rosinato, B.C. Nicholson, P. Pieronne, Destruction of cyanobacterial toxin by ozone, Ozone Sci. Eng. 20 (1998) 223–238.
[21] A. Shawwa, D.W. Smith, Kinetics of microcystin-LR oxidation by ozone, Ozone Sci. Eng. 23 (2001) 161–170.
[22] APHA-AWWA-WE.F, Standard Methods for the Examination of Water and Wastewater, 18th ed., American Public Health Association, American Water Works Association, and Water Environment Federation, Washington, DC, USA, 1992.
[23] M. Gamal El-Din, D.W. Smith, F. Al Momani, W. Wang, Oxidation of resin and fatty acids by ozone: Kinetics and toxicity study, Water Res. 40 (2006) 392–400.
[24] Olis, On-Line Instrument System Inc., 1998. The Olis RSM 1000 Operating System Users' Manual, Version VII.
[25] A.I. Vogel, A Text-book of Quantitative Inorganic Analysis Inculding Elementary Instrumental Analysis, third ed., Longmans, Green and Co. Ltd., London, UK, 1961, p. 363.
[26] W.W. Carmichael, The cyanotoxins. Advances in botanical research: incorporating, Adv. Plant Pathol. 27 (1997) 211–256.
[27] K. Himberg, A.-M. Keijola, L. Hiisvirta, H. Pyysalo, K. Sivonen, The effect of water treatment processes on the removal of hepatotoxins from Microcystis and Oscillatoria cyanobacteria: a laboratory study, Water Res. 23 (8) (1989) 979–984.
[28] J. Rositano, B. Nicholson, P. Pieronne, Destruction of cyanobacterial toxins by ozone, Ozone Sci. Eng. 20 (1998) 223–238.
[29] S. Staehelin, J. Hoigne, Mechanism and kinetics of decomposition of ozone in water in the presence of organic solutes, Vom Wasser 61 (1983) 337–344.
[30] B. Langlais, D.A. Reckhow, D.R. Brink, Ozone in Water Treatment. Application and Engineering, Lewis Publishers, Chelsea, Michigan, 1991.
[31] M. Trapido, Y. Veressinina, J.K. Hentunen, A. Hirvonen, Ozonation of chlorophenols: kinetics, by-products and toxicity, Environ. Technol. 18 (1997) 325–332.
[32] K. Abe, K. Tanaka, Fe^{3+} and UV-enhanced ozonation of chlorophenolic compounds in aqueous medium, Chemosphere 35 (12) (1999) 2837–2847.
[33] S. Amiri, R. James, R. Stephen, The use of iron in advanced oxidation processes, J. Adv. Oxid. Technol. 1 (1) (1996) 18–25.
[34] J. De Laat, H. Gallard, Catalytic decomposition of hydrogen peroxide by Fe(III) in homogeneous aqueous solution: mechanism and kinetic modeling, Environ. Sci. Technol. 33 (1999) 2726–2732.
[35] E. Neyens, J. Baeyens, A review of classic Fenton's peroxidation as an advanced oxidation technique, J. Hazard. Mater. 98 (1–3) (2003) 33–50.
[36] S. Esplugas, P.L. Yue, M.I. Pervez, Degradation of 4-chlorophenol by photolytic oxidation, Water Res. 28 (1994) 1323–1328.